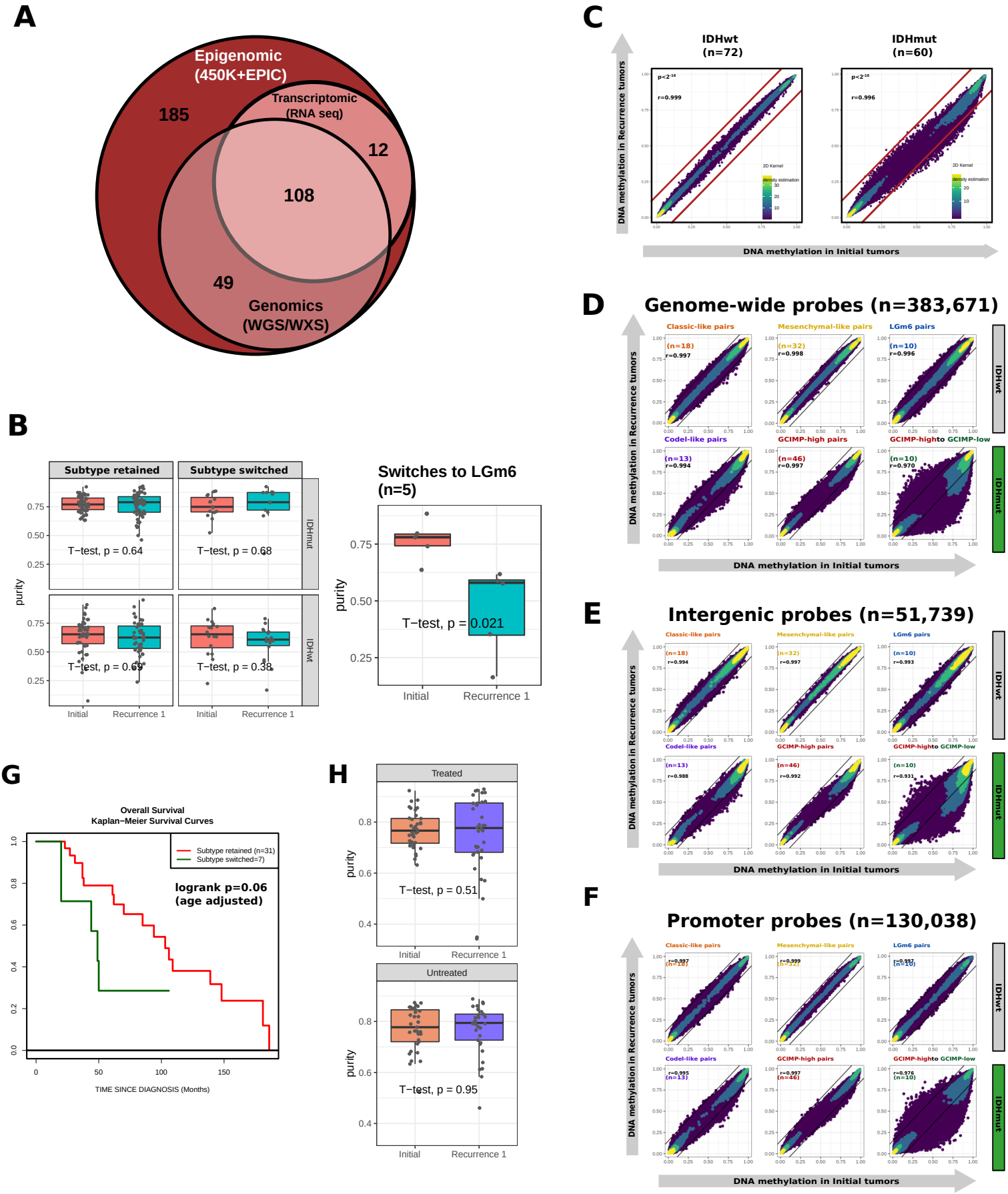

Figure S1. Longitudinal epigenomic changes of matched initial and recurrent gliomas, related to Figure 2. A) Venn diagram of DNA methylation samples which were profiled with genomics (WGS/WXS) and/or RNAseq. B) Tumor purity of GLASS samples who retained and switched TCGA subtypes, stratified by initial/recurrent and IDH mutation status. Each box represents quartiles, the center line represents the median of each group. The whiskers represent absolute range. C) Overall genome-wide DNA methylation correlation between initial and recurrent tumors, stratified by IDH mutation status. D/E/F) Overall DNA methylation correlation between initial and recurrent tumors of different glioma subtypes, by CpG probe genomic location: C, genome-wide; D, probes located in intergenic regions, and E, CpG probes located in promoters of genes. G) Overall survival analysis of IDHmut GCIMP-high gliomas of the GLASS International cohort stratified by subtype change status, referent to Table S3A. H) Tumor purity of treated and non-treated patients, stratified by initial/recurrent status. Each box represents quartiles, the center line represents the median of each group. The whiskers represent absolute range.

Figure S2

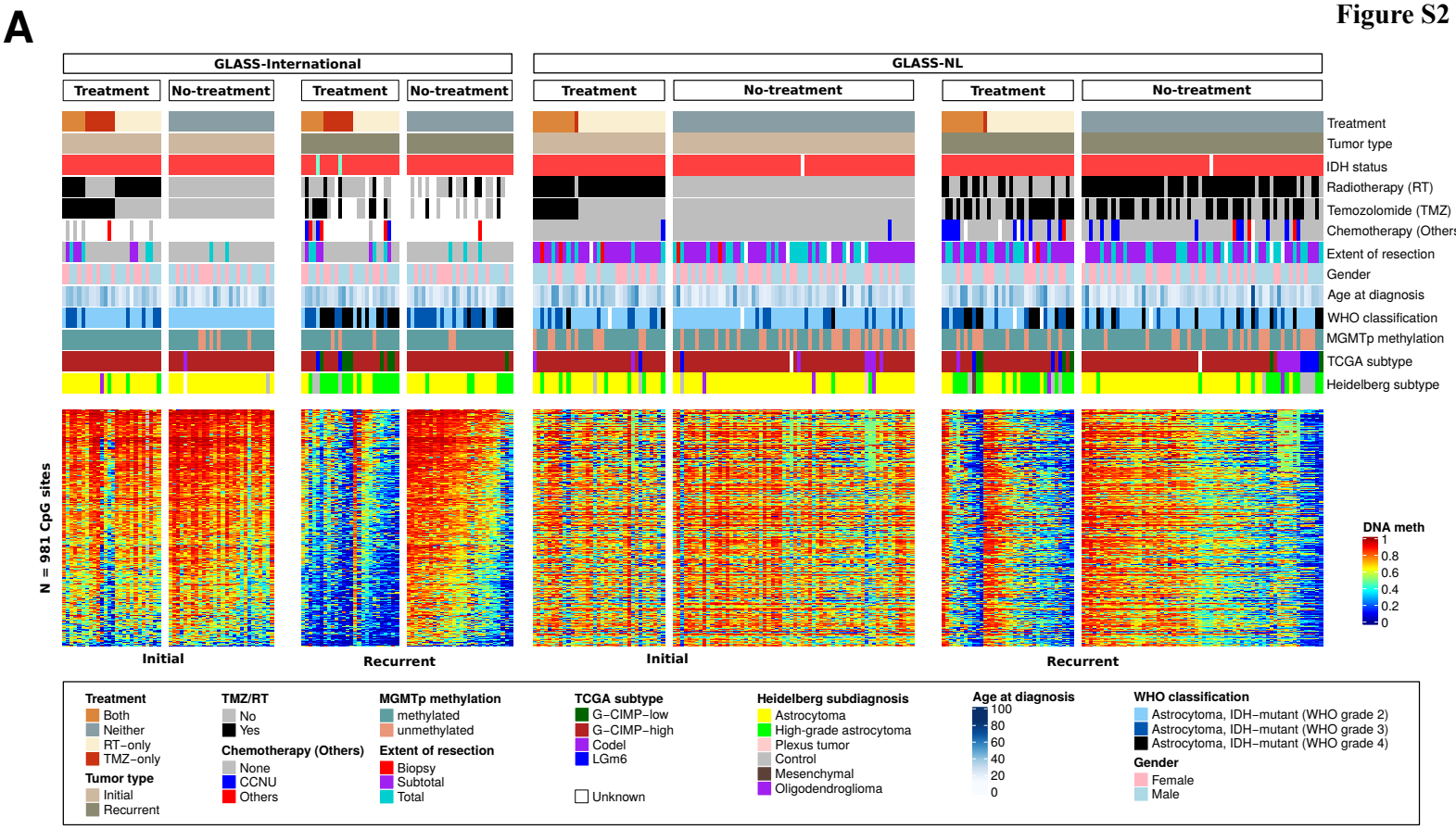
A
GLASS-International
GLASS-NL
Treatment
No-treatment
Tumor type
IDH status
Radiotherapy (RT)
Temozolomide (TMZ)
Chemotherapy (Others)
Extent of resection
Gender
Age at diagnosis
WHO classification
MGMTp methylation
TCGA subtype
Heidelberg subtype
N = 981 CpG sites
Initial
Recurrent
DNA meth
Both
Neither
RT−only
TMZ−only
No
Yes
None
CCNU
Others
methylated
unmethylated
Biopsy
Subtotal
Total
G−CIMP−low
G−CIMP−high
Codel
LGm6
Unknown
Astrocytoma
High-grade astrocytoma
Plexus tumor
Control
Mesenchymal
Oligodendroglioma
Astrocytoma, IDH−mutant (WHO grade 2)
Astrocytoma, IDH−mutant (WHO grade 3)
Astrocytoma, IDH−mutant (WHO grade 4)
Female
Male

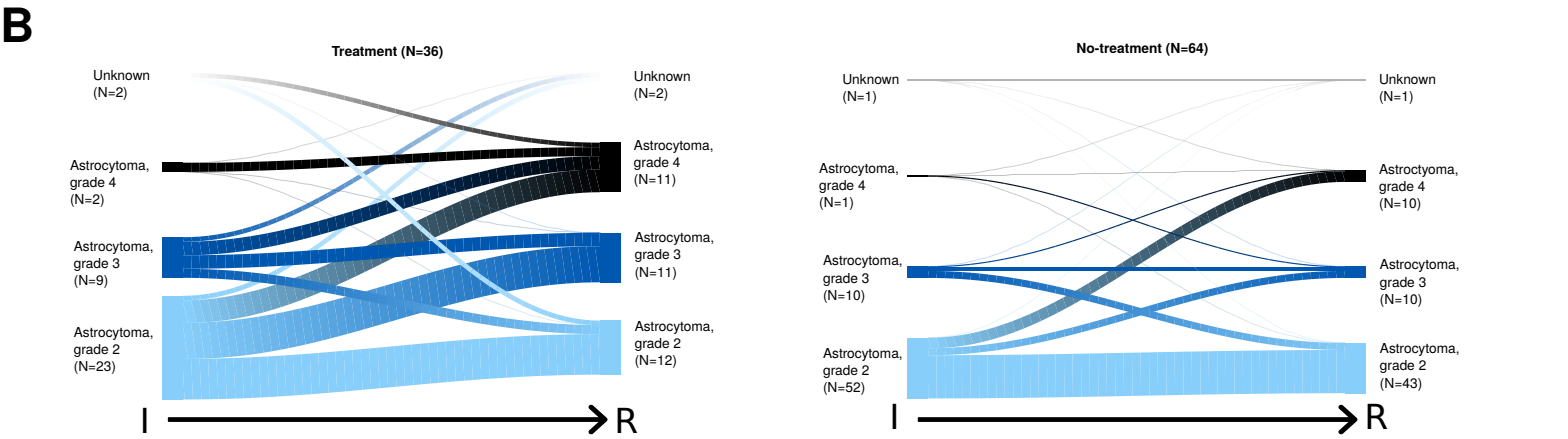
B
Treatment (N=36)
No-treatment (N=64)
Unknown (N=2)
Astrocytoma, grade 4 (N=2)
Astrocytoma, grade 3 (N=9)
Astrocytoma, grade 2 (N=23)
Astrocytoma, grade 4 (N=11)
Astrocytoma, grade 3 (N=11)
Astrocytoma, grade 2 (N=12)
Unknown (N=1)
Astrocytoma, grade 4 (N=1)
Astrocytoma, grade 3 (N=10)
Astrocytoma, grade 2 (N=52)
Astrocytoma, grade 4 (N=10)
Astrocytoma, grade 3 (N=10)
Astrocytoma, grade 2 (N=43)
I
R

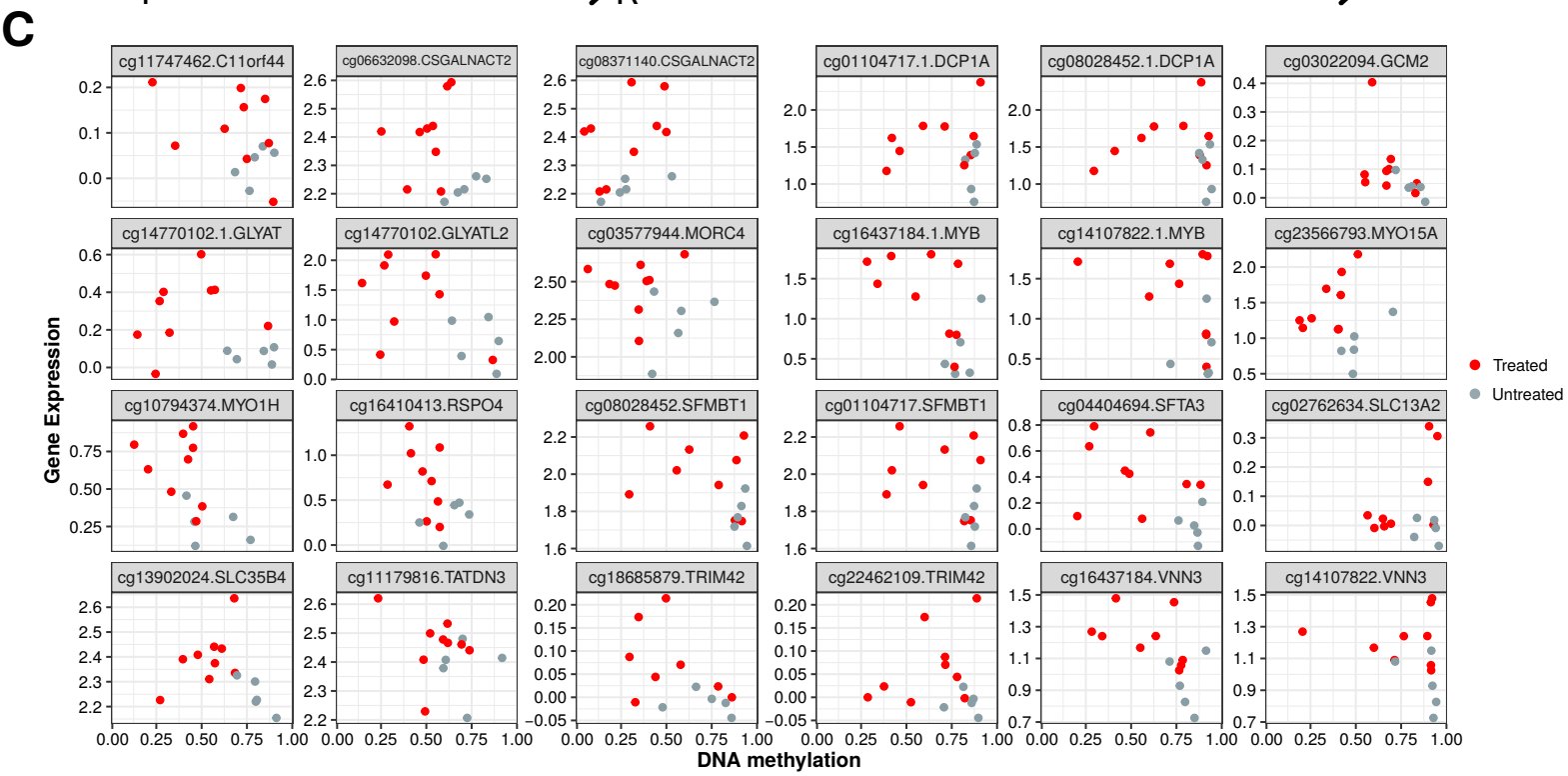
C
cg11747462.C11orf44
cg06632098.CSGALNACT2
cg08371140.CSGALNACT2
cg01104717.1.DCP1A
cg08028452.1.DCP1A
cg03022094.GCM2
cg14770102.1.GLYAT
cg14770102.GLYATL2
cg03577944.MORC4
cg16437184.1.MYB
cg14107822.1.MYB
cg23566793.MYO15A
cg10794374.MYO1H
cg16410413.RSPO4
cg08028452.SFMBT1
cg01104717.SFMBT1
cg04404694.SFTA3
cg02762634.SLC13A2
cg13902024.SLC35B4
cg11179816.TATDN3
cg18685879.TRIM42
cg22462109.TRIM42
cg16437184.VNN3
cg14107822.VNN3
Gene Expression
DNA methylation
Treated
Untreated

Figure S2. DNA methylation loss is associated with malignant progression of glioma after standard treatment in the validation cohort: GLASS-NL, related to Figure 3. A) Heatmap of DNA methylation data. Analysis using astrocytoma-only samples from GLASS-International cohort identified 981 CpG probes that are associated with treatment astrocytomas IDHmut paired glioma samples. Samples from the validation cohort are also shown. Samples are stratified by cohort, initial/recurrent status and treatment status. Column-wise represents glioma samples, row-wise represents CpG probes. DNA methylation beta-values range from 0 (low) to 1 (high). Additional tracks are included at the top of the heatmaps to identify each sample membership within separate cluster analysis. B) Evolution of tumor histology (2021 WHO classification) of the validation cohort (GLASS-NL) after treatment compared to non-treated gliomas. C) Scatter plot of 24 CpG-gene pairs epigenetically regulated genes after treatment in IDHmut gliomas.

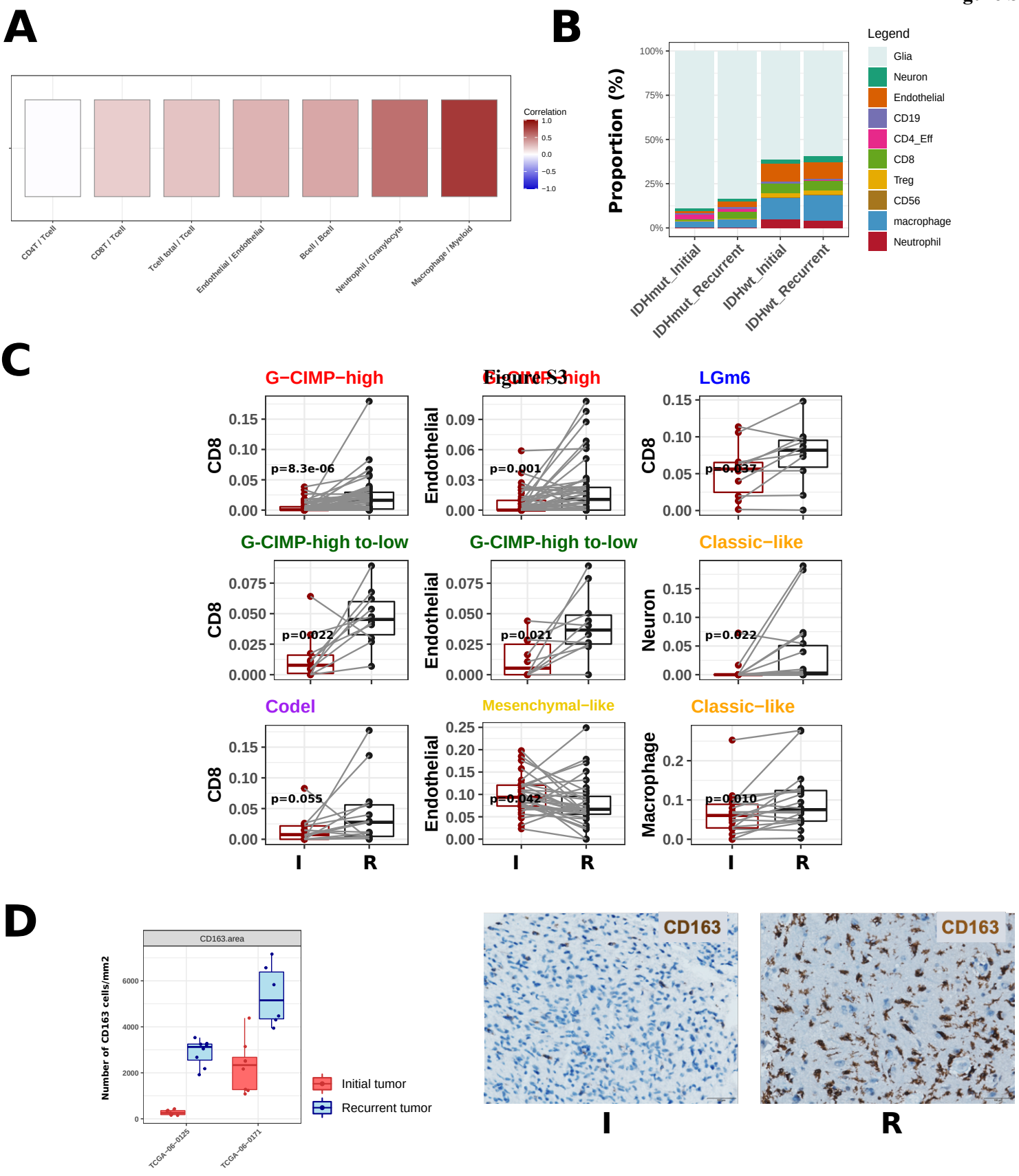

Figure S3. Glioma subtypes present different tumor microenvironments and it changes overtime, related to Figure 4. A) Correlation between cell composition estimated by DNA methylation and by gene expression. B) Barplots of the estimated median infiltration of specific cell types as a proportion of all cell types (range scaled from 0 to 100%) in 132 glioma tumors, divided by recurrent and IDH mutation status. C) Cell type proportion (range scaled from 0 to 100%) in samples originating from the matched initial and recurrent tumors, divided by molecular subtypes. All comparisons (initial vs. recurrence, by subtype, for the specified cell population) are statistically significant ($P < 0.05$). p-values calculated using a paired Wilcoxon rank-sum test. Matched initial and recurrent tumors are linked by the lines. D) Representative immunohistochemical staining for CD163 marker protein in two individual patients with changing levels of tumor-infiltrating immune cells between initial and recurrent tumors.

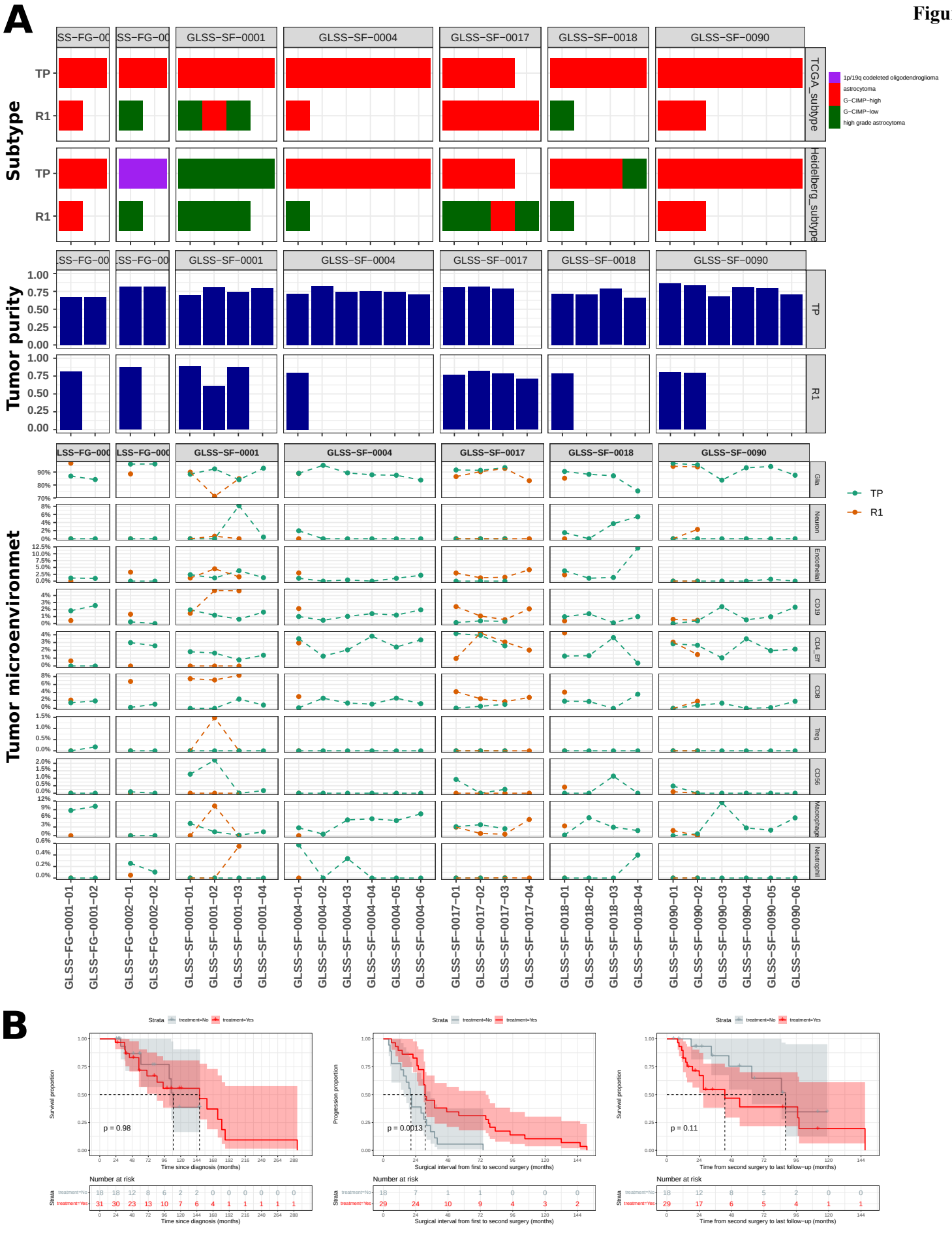

Figure S4. Glioma subtypes present different tumor microenvironments and it changes overtime, related to Figure 4. A) Overview of subtype, tumor purity and tumor microenvironment (TME) of the 7 GLASS patients which have multiple fragments from the same surgery available. B) Overall survival and surgical interval analysis of IDHmut gliomas grade 2 for the GLASS International cohort.